

# Critical current characteristics in MgB<sub>2</sub> bulks

M. Kiuchi <sup>a,1</sup>, H. Mihara <sup>a</sup>, K. Kimura <sup>a</sup>, T. Haraguchi <sup>a</sup>,  
E.S. Otabe <sup>a</sup>, T. Matsushita <sup>a</sup>, A. Yamamoto <sup>b</sup>, J. Shimoyama <sup>b</sup>,  
K. Kishio <sup>b</sup>

<sup>a</sup>*Faculty of Computer Science and Systems Engineering,  
Kyushu Institute of Technology, 680-4 Kawazu, Iizuka 820-8502, Japan*

<sup>b</sup>*Department of Superconductivity, University of Tokyo,  
7-3-1 Hongo, Bunkyo-ku, Tokyo 113-8556, Japan*

---

## Abstract

The effects of low temperature sintering and C-doping on the critical current density of MgB<sub>2</sub> superconductor was investigated and the obtained results were compared with the theoretical results of the flux creep-flow model. The critical current density increased by these treatments over a wide range of magnetic fields. It is proposed that the improvement of the critical current density at low magnetic fields comes from the reduction of the grain size in the specimen sintered at low temperatures and from the increase in the elementary pinning force of grain boundaries in the C-doped specimens. On the other hand, the improvement of the critical current density at high fields is mainly caused by the enhancement of the upper critical field due to the electron scattering by grain boundaries and C atoms.

*Key words:* MgB<sub>2</sub>, critical current density, irreversibility field, upper critical field, flux creep-flow mode

*PACS:* : 74.70.Ad; 74.62.Dh; 74.25.Qt; 74.25.Sv

---

<sup>1</sup> Corresponding author. Postal address: Department of Computer Science and Electronics, Kyushu Institute of Technology, 680-4 Kawazu, Iizuka 820-8502, Japan  
Phone/fax: +81-948-29-7661  
E-mail address: kiuchi@cse.kyutech.ac.jp (M. Kiuchi)

## 1 Introduction

Since  $\text{MgB}_2$  has a high critical temperature ( $T_c$ ) of 39 K [1], one can expect its application at around 20 K at which cryo-cooling systems are available. Many efforts have been done for improvement of the critical current properties of this material in this temperature region. It is empirically known that grain boundaries are dominant pinning centers which determine the critical current density. Hence, it is desired to reduce the grain size for achievement of high critical current density.

Recently, it was reported that the critical current density at high temperatures and high magnetic fields can be improved by addition of elements such as SiC [2]. In this case, B sites are partly substituted by C atoms and the superconductor becomes “dirty”. The improvement of the critical current density is considered to be attributed either to an increase in the upper critical field,  $B_{c2}$ , or to an increase in the flux pinning force of grain boundaries. However, it has not yet been clarified which contributes mainly to the improvement.

On the other hand, it is also known that the critical current density is also improved by the sintering at low temperatures. This improvement seems to be ascribed to the decrease in the grain size. However, there is another possibility that this comes indirectly from the increase in  $B_{c2}$  due to strong electron scattering by high density of grain boundaries. Therefore, it is necessary to examine the mechanism of the improvement of the critical current density even in this case.

In this work, the effects of sintering temperature and C-doping on the critical current density are investigated in a high temperature region. The obtained

results are compared with the theoretical results of the flux creep-flow model.

## 2 Experiments

The specimens were prepared by PICT (powder-in-closed-tube) method. The raw powders are put into the SUS316 tube sealed by uniaxial pressing. After pressing the other end of the tube, the part of the tube filled with the raw powder is pressed in to the tape shape. The pressed tube was sealed in an evacuated quartz ampoule to prevent oxidation of the SUS316 tube, sintered 600–950°C for 3–24h, and then quenched to room temperature [3]. Specimens #1 and #2 are nondoped specimens prepared in different conditions of the sintering temperature and time. Specimens #3 and #4 are doped with B<sub>4</sub>C and SiC, respectively. The specifications of specimens are listed in Table 1.

The critical current density was estimated from the hysteresis width of the magnetization using a SQUID magnetometer(Quantum Design: MPMS-7). The irreversibility field was defined by the magnetic field at which the obtained critical current density was reduced to  $1 \times 10^6$  A/m<sup>2</sup>.

## 3 Discussion

The temperature dependence of the critical current density of the four specimens at high temperatures is shown in Fig. 1(a), (b), (c) and (d). The irreversibility field,  $B_i$ , of the four specimens is shown in Fig. 2. It is found from these results that the critical current density and the irreversibility field are significantly improved by the low temperature sintering and addition of C. The best results are obtained for the SiC-doped specimen.

The high critical current density in specimen #2 at low magnetic fields seems to be caused by a small size of grain, i.e., a higher density of pinning centers, since its value is not influenced by  $B_{c2}$ . In addition, the critical current density at high fields is also improved. This could be ascribed either to the enhancement of pinning force or to the enhancement of  $B_{c2}$ .

The critical current density at low magnetic fields in C-doped specimens also increases. This improvement is considered to be caused by the enhanced flux pinning strength by grain boundaries, since the grain size is not appreciably reduced by addition of SiC and  $B_4C$ . The reason for the enhancement of the grain boundary pinning may be the change in the impurity parameter by the electron scattering by C atoms in honeycomb B structure. The higher critical current density in the SiC-doped specimen is ascribed to the high substitution rate of C [4]. On the other hand, the critical current density at high fields is also improved by the doping. It is also ascribed either to the enhancement of pinning force or to the enhancement of  $B_{c2}$ .

Here we will discuss the flux pinning mechanism of these specimens. The scaled curves of the pinning force density for specimens #1 and #4 are shown in Fig. 3(a) and (b), respectively. It is found that the scaling law of Kramer type of  $F_p \propto b^{1/2}(1 - b)^2$  fits well, where the  $b$  is the magnetic field normalized by the irreversibility field. This magnetic field dependence of  $F_p$  is known for the pinning by grain boundaries as in  $Nb_3Sn$ . Similar scaling is obtained also for specimens #2 and #3. Hence, the pinning mechanism of all specimens is considered to be the grain boundary pinning.

Next we will discuss the flux pinning properties of these tapes in more detail by analysing the observed results with the flux creep-flow model [5]. According

to the model, the flux pinning potential,  $U_0$ , is given by

$$U_0 = \frac{0.835g^2k_B J_{c0}^{1/2}}{(2\pi)^{3/2}B^{1/4}}, \quad (1)$$

where  $J_{c0}$  is the virtual critical current density in the creep free case and  $g^2$  is the number of flux lines in the flux bundle. Here, the magnetic field and temperature dependence of  $J_{c0}$  is assumed as

$$J_{c0} = A \left(1 - \frac{T}{T_c}\right)^m B^{\gamma-1} \left(1 - \frac{B}{B_{c2}}\right)^2, \quad (2)$$

where,  $A$ ,  $m$ ,  $\gamma$  and  $\delta$  are pinning parameters. The distribution of the pinning strength is approximated by that of  $A$  in Eq. (2) as

$$f(A) = K \exp \left[ -\frac{(\log A - \log A_m)^2}{2\sigma^2} \right], \quad (3)$$

where  $A_m$  is the most probable value of  $A$ ,  $\sigma^2$  is a parameter representing the distribution width and  $K$  is a constant. The parameters  $A_m$ ,  $m$ ,  $\gamma$ ,  $\sigma^2$  and  $g^2$  are determined so as to fit the experimental and theoretical results of the critical current density. Further details of the numerical calculation is presented in Ref. [6]. On the other hand, the upper critical field,  $B_{c2}(0)$ , has the possibility to change with the doping and heat treatment. Therefore,  $B_{c2}(0)$  is used as an adjusting parameter in this analysis. The superconducting and pinning parameters used in the numerical calculation are shown in Table 2. The calculated results of critical current density and irreversibility field are compared with the experimental results in Figs. 1 and 2, respectively. It is seen that the agreement is satisfactory.

Here, each contribution of the upper critical field and the pinning force to the critical current density and the irreversibility field will be discussed using the above numerical results. It is found from Table 2 that the parameters other

than  $A_m$  and  $B_{c2}(0)$  used for the theoretical analysis are approximately the same among the specimens. Since the  $A_m$  value increases by the low temperature sintering and the C-doping in specimens #2–4, the flux pinning force is strengthened as discussed above. That is, the number density is increased in specimen #2 and the pinning force by grain boundaries is increased in specimens #3 and #4. If these results are compared in more detail, the reduction in the grain size seems to be more effective. As for the elementary pinning force of grain boundaries, it is necessary to search the optimum condition for the electron scattering by C atoms for further enhancement.

The flux pinning properties at high magnetic fields are also influenced by  $B_{c2}$ . These properties are directly associated with the irreversibility field. According to the flux creep theory [5], the relationship between the flux pinning strength and the irreversibility field is  $B_i \propto A_m^{1/3}$ , when  $B_i$  is sufficiently lower than  $B_{c2}$ . If we compare specimens #1 and #2,  $A_m$  increases by a factor of 2 and hence,  $B_i$  is expected to increase by a factor of 1.26. The observed enhancement factor of the irreversibility field at  $T/T_c = 0.5$  of specimen #2 from specimen #1 is about 1.73. Hence, it is concluded that the effect of the enhancement of  $B_{c2}$  is larger than that of the enhancement of the pinning strength for the improvement of the irreversibility field.

In specimens #3 and #4 the improvement of the irreversibility field mostly comes from the enhancement of the upper critical field. Even if it is assumed that only  $B_{c2}(0)$  in specimen #1 is changed to 18.4 T without changes in other parameters, the irreversibility field is estimated to be 5.25 T at  $T = 20$  K, which is approximately equal to the observed result for specimen #3. This supports the above speculation that the improvement of the critical current density in a high field region is mainly attributed to the improvement of the

upper critical field.

Comparing the effects of low temperature sintering and C-doping, the low temperature sintering gives a better performance at low magnetic fields. That is, the reduction in the grain size is more effective. On the other hand, the C-doping derives a better performance at high magnetic fields. Hence, the C-doping is more effective than grain boundaries for the reduction of the coherence length by electron scattering.

#### **4 Summary**

The effects of low temperature sintering and C-doping on the critical current density of  $\text{MgB}_2$  superconductor at high magnetic fields are investigated. The improvement of the critical current density at low magnetic fields comes from the enhancement of the flux pinning strength: i.e., the increase in the pin number density in the specimen sintered at low temperatures and the increase in the elementary pinning force of grain boundaries in the C-doped specimens. On the other hand, the improvement of the critical current density at high fields is mainly caused by the enhancement of the upper critical field due to additional electron scattering by grain boundaries and C atoms.

## References

- [1] J. Nagamatsu, N. Nakagawa, T. Muranaka, Y. Zenitani, J. Akimitsu, *Nature* **410** (2001) 63.
- [2] S. X. Dou, S. Soltanian, J. Harvat, X. L. Wang, S. H. Zhou, M. Ionescu, H. K. Liu, P. Munroe, M. Tomsic, *Appl. Phys. Lett.* **81** (2002) 3419.
- [3] A. Yamamoto, J. Shimoyama, S. Ueda, Y. Katsura, S. Horii, K. Kishio, *Supercond. Sci. Technol.* **17** (2004) 921.
- [4] S. Lee, T. Masui, A. Yamamoto, H. Uchiyama, S. Tajima, *Physica C* **412–414** (2004) 31.
- [5] N. Ihara, T. Matsushita, *Physica C* **257** (1996) 223.
- [6] M. Kiuchi, K. Noguchi, T. Matsushita, T. Kato, T. Hikata, K. Sato, *Physica C* **278** (1997) 62.

Table 1: Specifications of specimens.

sample	composition	sintering condition	$T_c$ [K]
#1	MgB <sub>2</sub>	950°C, 12h	38.9
#2	MgB <sub>2</sub>	600°C, 24h	38.1
#3	MgB <sub>1.5</sub> (B <sub>4</sub> C) <sub>0.1</sub>	850°C, 3h	35.6
#4	MgB <sub>1.80</sub> (SiC) <sub>0.2</sub>	850°C, 3h	35.6

Table 2. Pinning parameters used in the theoretical calculation.

specimen	$A_m$	$\sigma^2$	$m$	$\gamma$	$g^2$	$B_{c2}(0)$ [T]
#1	$4.00 \times 10^9$	0.001	1.5	0.5	1.2	9.80
#2	$8.00 \times 10^9$	0.001	1.5	0.5	1.2	14.5
#3	$6.20 \times 10^9$	0.001	1.5	0.5	1.2	17.9
#4	$6.00 \times 10^9$	0.001	1.5	0.5	1.6	18.4

Figure captions

Fig. 1. Critical current density of specimens (a) #1, (b) #2, (c) #3 and (d) #4. The solid lines show the theoretical results of the flux creep-flow model.

Fig. 2. Irreversibility field of each specimen. The solid lines show the theoretical results of the flux creep-flow model.

Fig. 3. Scaling curves of the pinning force density for specimens (a) #1 and (b) #4.

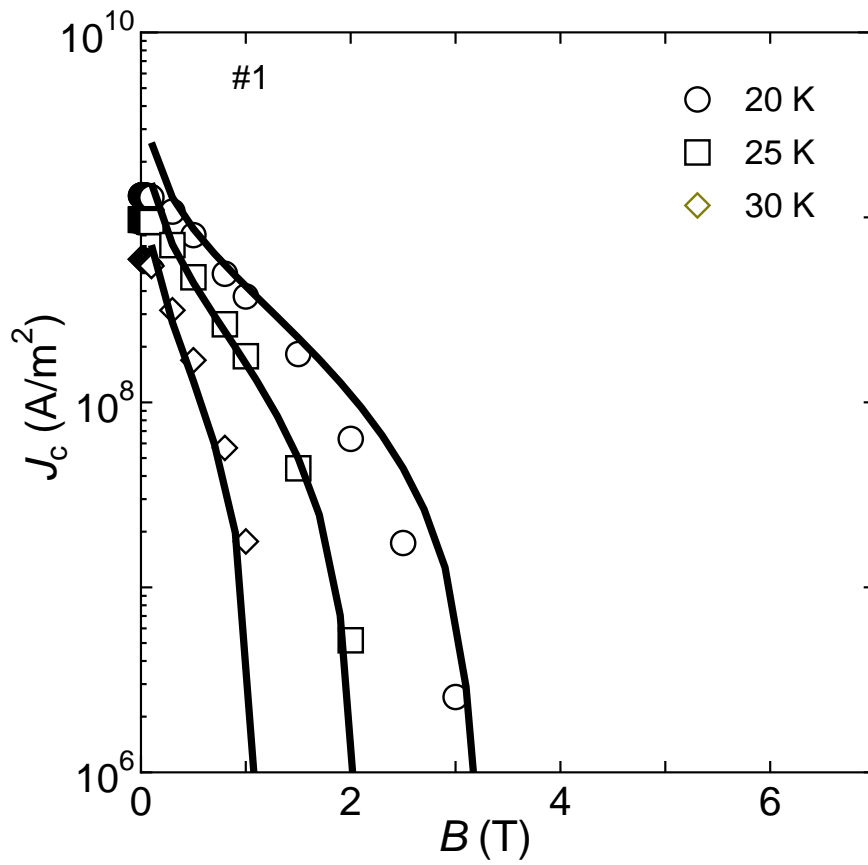


Figure 1(a): M. Kiuchi *et al.*/BLP-46/ ISS2005

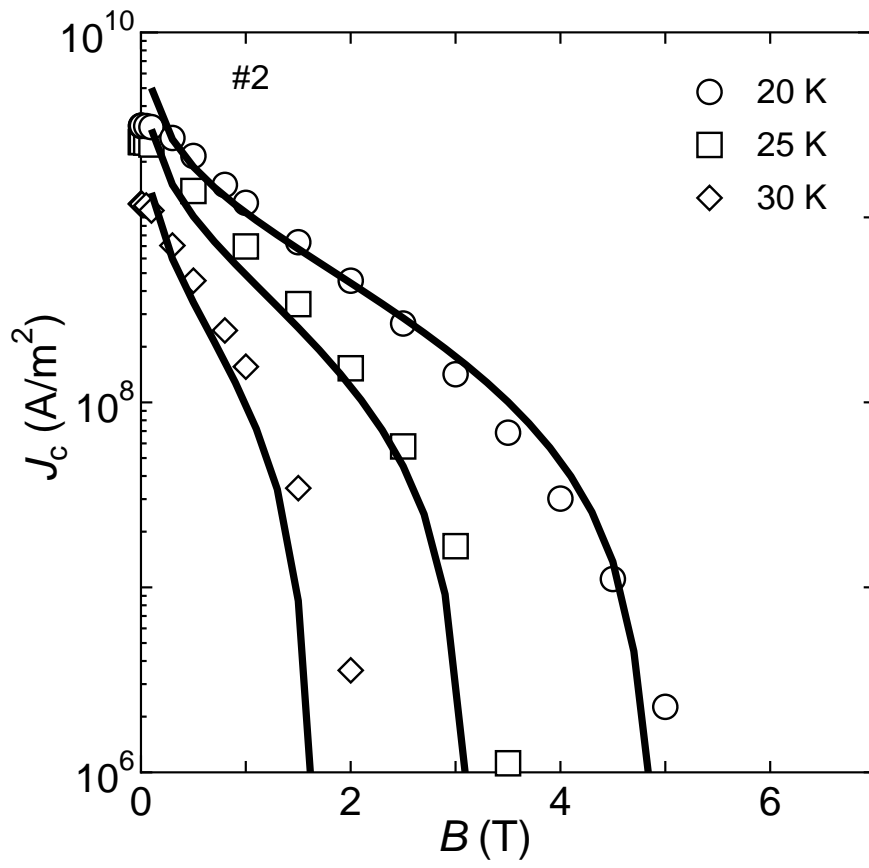


Figure 1(b): M. Kiuchi *et al.*/BLP-46/ ISS2005

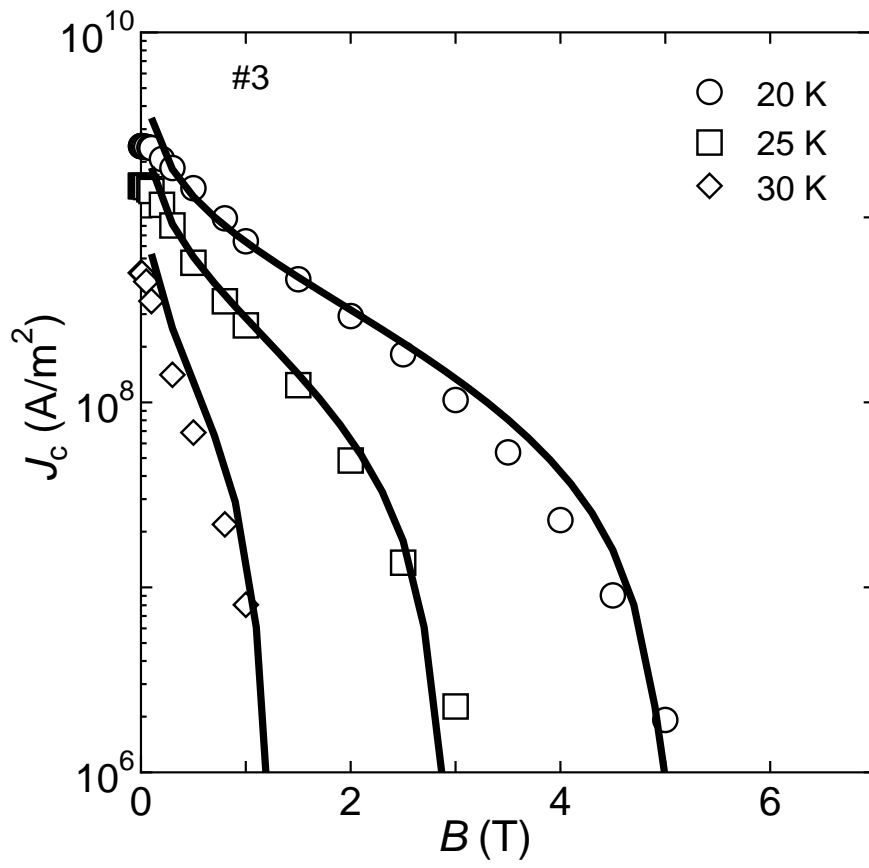


Figure 1(c): M. Kiuchi *et al.*/BLP-46/ ISS2005

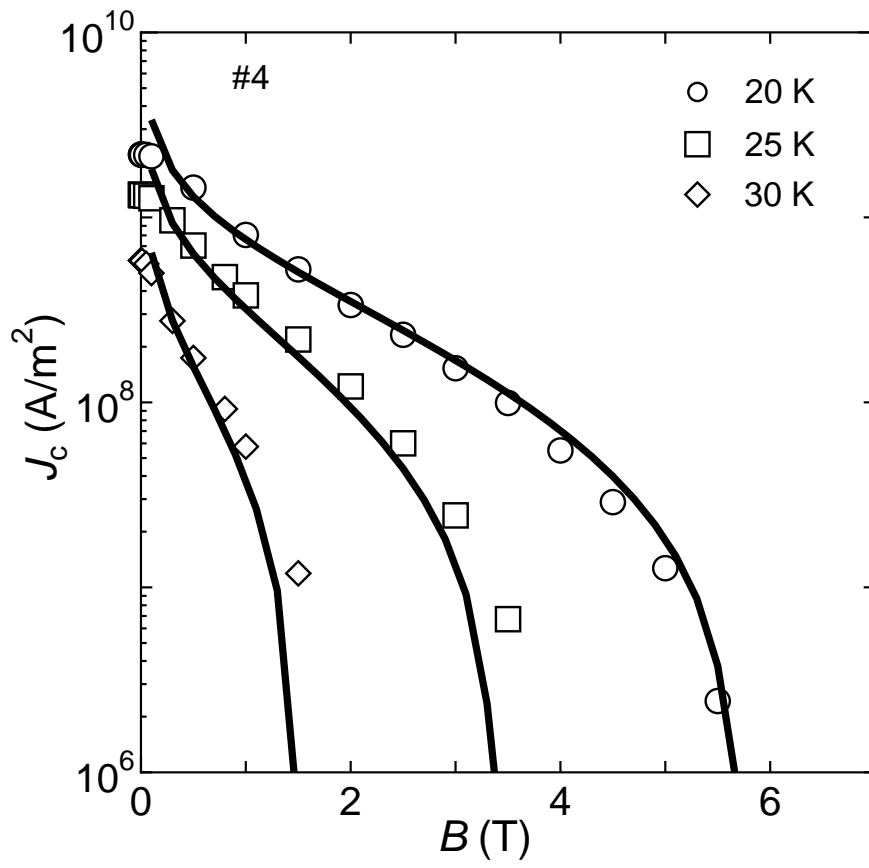


Figure 1(d): M. Kiuchi *et al.*/BLP-46/ ISS2005

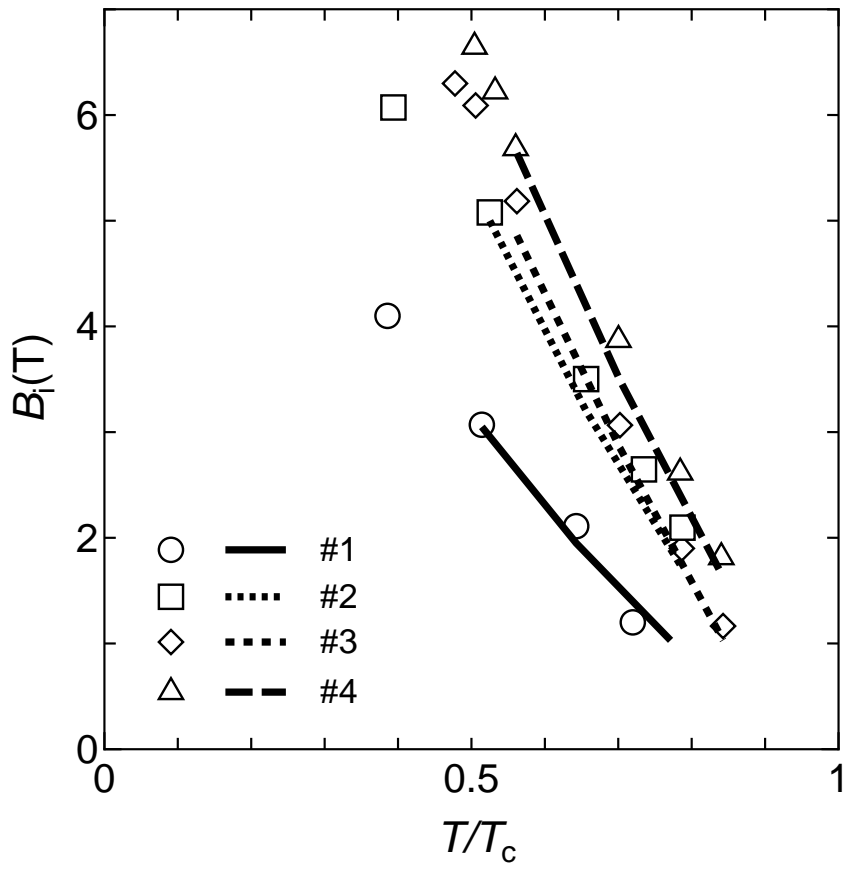


Figure 2: M. Kiuchi *et al.*/BLP-46/ ISS2005

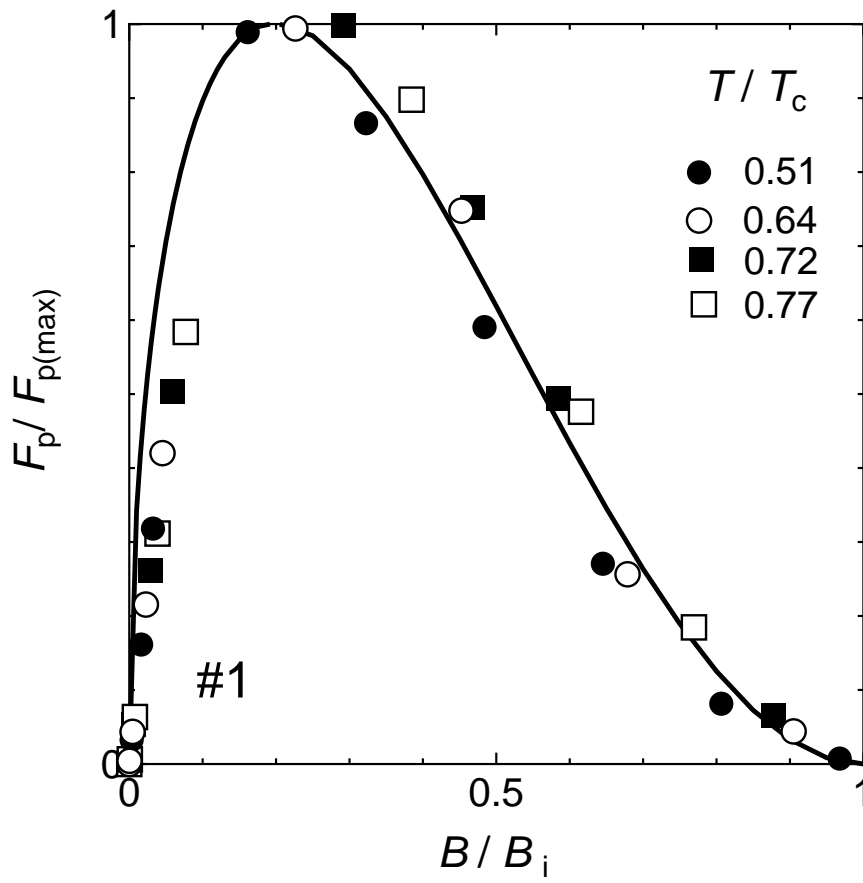


Figure 3(a): M. Kiuchi *et al.*/BLP-46/ ISS2005

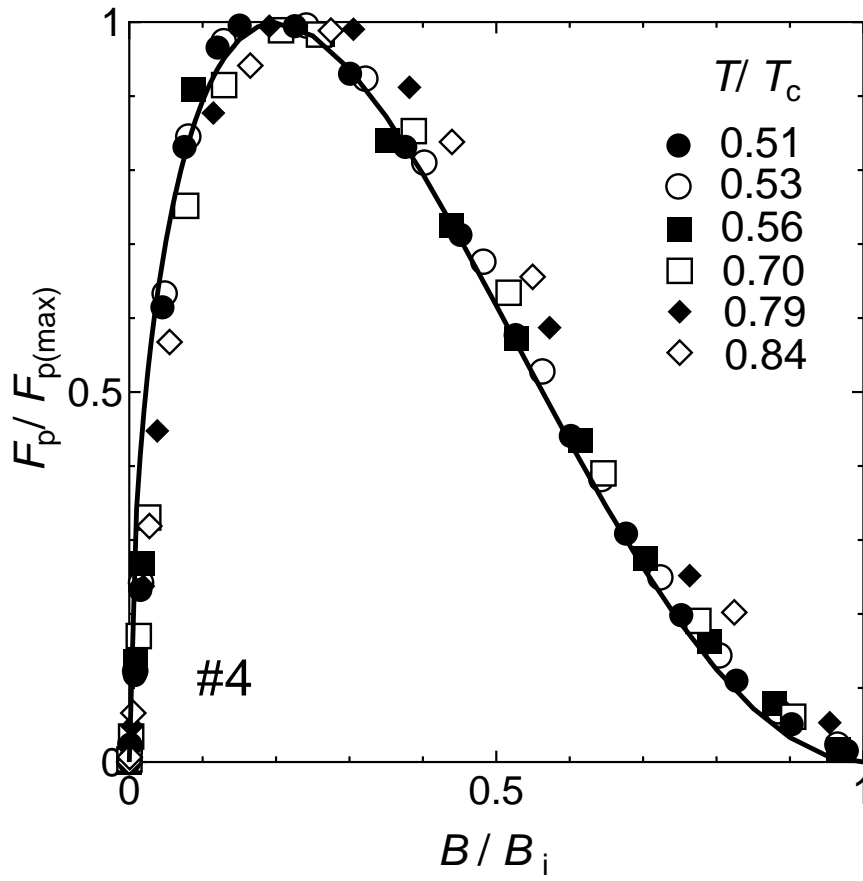


Figure 3(b): M. Kiuchi *et al.*/BLP-46/ ISS2005